CrossMark

Screening and identification of small molecule inhibitors of ErbB2-induced invasion

D.M. Brix[a,1], B. Rafn[a,1], K. Bundgaard Clemmensen[a], S.H. Andersen[a], N. Ambartsumian[b], M. Jäättelä[a], T. Kallunki[a,*]

[a]Unit of Cell Death and Metabolism, Danish Cancer Society Research Center, Strandboulevarden 49, DK-2100 Copenhagen, Denmark
[b]Department of Neuroscience and Pharmacology, Faculty of Health Sciences, University of Copenhagen, Blegdamsvej 3B, DK-2200 Copenhagen N, Denmark

ARTICLE INFO

ABSTRACT

ERBB2 amplification and overexpression are strongly associated with invasive cancer with high recurrence and poor prognosis. Enhanced ErbB2 signaling induces cysteine cathepsin B and L expression leading to their higher proteolytic activity (zFRase activity), which is crucial for the invasion of ErbB2-positive breast cancer cells *in vitro*. Here we introduce a simple screening system based on zFRase activity as a primary readout and a following robust invasion assay and lysosomal distribution analysis for the identification of compounds that can inhibit ErbB2-induced invasion. With an unbiased kinase inhibitor screen, we identified Bohemine/Roscovitine, Gö6979 and JAK3 inhibitor VI as compounds that can efficiently decrease cysteine cathepsin activity. Using the well-established and clinically relevant ErbB1 and ErbB2 inhibitor lapatinib as a positive control, we studied their ability to inhibit ErbB2-induced invasion in 3-dimensional Matrigel cultures. We found one of them, JAK3 inhibitor VI, capable of inhibiting invasion of highly invasive ErbB2-positive ovarian cancer cells as efficiently as lapatinib, whereas Gö6979 and Roscovitine displayed more modest inhibition. All compounds reversed the malignant, ErbB2-induced and invasion-supporting peripheral distribution of lysosomes. This effect was most evident for lapatinib and JAK3 inhibitor VI and milder for Gö6979 and Roscovitine. Our results further showed that JAK3 inhibitor VI function was independent of JAK kinases but involved downregulation of cathepsin L. We postulate that the screening method and the verification experiments that are based on oncogene-induced changes in lysosomal hydrolase activity and lysosomal distribution could be used for identification of novel inhibitors of ErbB2-induced invasiveness. Additionally, we introduce a novel function for lapatinib in controlling malignant lysosomal distribution, that may also be involved in its capability to inhibit ErbB2-induced invasion *in vivo*.

© 2014 The Authors. Published by Elsevier B.V. on behalf of Federation of European Biochemical Societies. This is an open access article under the CC BY-NC-ND license (http://creativecommons.org/licenses/by-nc-nd/3.0/).

* Corresponding author. Tel.: +45 35 25 77 46.
  E-mail address: tk@cancer.dk (T. Kallunki).
 [1] These authors share equal authorship.

1. Introduction

Amplification of *ERBB2* oncogene and the consecutive overexpression of ErbB2 are observed in 20−30% of advanced human breast and ovarian adenocarcinomas (Baselga and Swain, 2009; Santarius et al., 2010; Slamon et al., 1989, 2001). Overexpression of the ErbB2 receptor tyrosine kinase leads to its auto-phosphorylation and activation of multiple downstream signaling networks that can drive cell proliferation, transformation, angiogenesis, invasion and metastasis (Brix et al., 2014; Holbro et al., 2003; Hynes and Lane, 2005). A most commonly expressed form of ErbB2 is the full-length 185 kid form. An alternative form of ErbB2, referred to as p95 ErbB2 that lacks the NH_2-terminal extracellular domain of ErbB2, is often expressed in aggressive breast cancers with lymph node metastasis and its expression is an independent prognostic factor for cases with significantly worse outcome predicting resistance to therapeutic ErbB2 inhibition (Molina et al., 2002; Scaltriti et al., 2007; Xia et al., 2011).

Three ErbB2-targeting drugs are mainly used to treat ErbB2-positive cancers. The humanized monoclonal antibody trastuzumab, which binds directly to the extracellular part of ErbB2 (Clynes et al., 2000), is currently used in combination with chemotherapeutic agents as the first line treatment for ErbB2-positive breast cancer. The second drug lapatinib is a small molecular compound tyrosine kinase inhibitor that targets the intracellular kinase domains of ErbB1 and ErbB2 and is used in combination with chemotherapeutic agents, with or without trastuzumab, mainly to treat trastuzumab resistant ErbB2-positive breast cancers (Blumenthal et al., 2013; Kumler et al., 2014). Clinical trials using trastuzumab or lapatinib to treat ErbB2-positive ovarian cancers have yet not been as successful and have failed approval by the European Medicine Agency (EMA) and the US Food and Drug Administration (FDA), even though the preceding preclinical studies had shown that lapatinib could be used efficiently for ovarian cancers expressing either N-terminally truncated p95 ErbB2 or full-length ErbB2 (Scaltriti et al., 2010). However, the third clinically approved ErbB2-targeting drug pertuzumab in combination with chemotherapeutic agents plays a beneficial role in the treatment of the ErbB2-positive ovarian cancer patients (Makhija et al., 2010), supporting the assumption that ErbB2 can also drive the malignancy of ovarian cancer.

Many ErbB2-positive breast cancer patients suffer from short-lived clinical responses due to primary or acquired secondary resistance (Moasser, 2007). For example, p95 ErbB2 is lacking the trastuzumab binding site and thus patients expressing p95 ErbB2 do not respond efficiently to trastuzumab treatment (Arribas et al., 2011). Moreover trastuzumab can induce ventricular dysfunction and heart failure (De Keulenaer et al., 2010). Long-time exposure to lapatinib is less cardiotoxic than trastuzumab (Perez et al., 2008), but acquired resistance can be reached within a year due to redundancy of metabolic signaling pathway components (Komurov et al., 2012). The potent cardiotoxicity and resistancy that are connected to currently used ErbB2-targeting agents identifies a critical need for the development of novel treatment options.

Elevated levels of cysteine cathepsins are associated with enhanced angiogenesis, invasion and metastasis of breast and ovarian cancers (Gocheva et al., 2006; Kirkegaard and Jaattela, 2009; Kobayashi et al., 1992; Kolwijck et al., 2010; Mohamed and Sloane, 2006; Nishikawa et al., 2004; Thomssen et al., 1995; Zhang et al., 2011). Upon secretion to the extracellular space, cysteine cathepsins can mediate the activation of urokinase plasminogen activator (uPA) and matrix metalloproteases (MMPs) (Bosc et al., 2001; Ke et al., 2006; Kobayashi et al., 1992; Yong et al., 2010; Zhang et al., 2011). Oncogene-driven invasive cell lines and tumors show lysosomal redistribution from the perinuclear position to the cellular periphery in comparison to their non-transformed counterparts (Fehrenbacher et al., 2008; Rafn et al., 2012; Victor and Sloane, 2007). The pericellular localization of lysosomes enables the secretion of lysosomal hydrolases into the extracellular space to promote matrix degradation and invasion (Sloane et al., 1994).

Activation of ErbB2 and lysosomal cysteine cathepsins B and L are strongly linked to ErbB2-positive, invasive breast cancer (Rafn et al., 2012). Significant positive correlation exists between the expression of cathepsins B and L and the ErbB2 status in primary human breast tumors. Recently a signaling network was identified that connects ErbB2 activation to upregulation of cysteine cathepsins B and L, pericellular localization of lysosomes and invasiveness of breast cancer cells in 3-dimensional (3D) Matrigel cultures (Rafn et al., 2012). The identified signaling network consists of serine threonine kinases PKCα, PAK4 (5 and 6), TGFβRI, TGFβRII, Cdc42BPβ and ERK2 (Rafn et al., 2012) as essential hubs mediating ErbB2-induced invasiveness and thus providing several potential targets for small molecule kinase inhibitor intervention. Inspired by this, we decided to use the assays and model systems developed in the study (Rafn et al., 2012) to set up a robust screening system for the identification of novel compounds that can inhibit ErbB2-induced invasiveness. Studies of small molecular weight compound kinase inhibitors have resulted in promising therapeutical compounds and a substantial number of protein kinase inhibitors have reached the clinic and approval by FDA as anti-cancer agents during recent years (Chahrour et al., 2012; Grant, 2009). Thus, we set up a small-scale test screen using the Calbiochem Inhibitor Select kinase inhibitor libraries I and II and used the activity of lysosomal cysteine cathepsins (zFRase activity) as the readout. We speculated that by using zFRase activity as a readout, we may also be able to identify compounds that can inhibit invasion-promoting events downstream of the receptor. To assess the screening results more extensively, we established a 3D invasion model system for a highly invasive ErbB2-positive ovarian cancer cell line SK-OV3 and its more aggressive subline SK-OV3.ip1. In the consecutive validation work we used lapatinib as a positive control. In 3D Matrigel invasion and immunofluorescence experiments we found lapatinib, as well as all the identified novel compounds Roscovitine, Gö6979 and JAK3 inhibitor VI to have profound effects on invasion and on lysosomal trafficking, a phenomenon that has been linked to cancer invasion.

2. Materials and methods

2.1. Antibodies, reagents and chemicals

Following antibodies were used: Cathepsin B (AB-1) from Merck Chemicals; Cathepsin B from Ekkehard Weber; ErbB2 form Thermo Scientific; phosphor-ErbB2 (Tyr1221/1222), JAK1, JAK2, JAK3, STAT3, phosphor-STAT3 (Tyr727) and Bax from Cell Signaling Technology; GAPDH from AbD Biogenesis; Hsc70 (N69a) from Boris Marqulis; LAMP-2 from Hybridoma Bank Iowa; PCNA from DAKO; α-tubulin from Abcam. Kinase inhibitor libraries InhibitorSelect I and II (Calbiochem) were used to screen compounds that can decrease zFRase activity. Additionally, following inhibitor compounds were used: Lapatinib Ditosylate (Santa Cruz) and Bohemine, Roscovitine, Gö6979 and JAK3 inhibitor VI (Calbiochem). Following lentiviral shRNAs from Sigma Aldrich were used:

ERBB2 (1): CCGGATCACAGGTTACCTATACATCTCGAGATG TATAGGTAACCTGTGATCTTTTTG; ERBB2 (2): CCGGAAGTA CACGATGCGGAGACTCTCGAGAGTCTCCGCATCGTGTACTTC TTTTTG; ERBB2 (3): CCGGTGTCAGTATCCAGGCTTTGTACTC GAGTACAAAGCCTGGATACTGACATTTTTG; CTSB (1): CCGGG CTGGTCAACTATGTCAACAACTCGAGTTGTTGACATAGTTGA CCAGCTTTTT; CTSB (2): CCGGCCAGAGAGTTATGTTTACC GACTCGAGTCGGTAAACATAACTCTCTGGTTTTT; CTSL1 (1): CCGGGCTGGTCAACTATGTCAACAACTCGAGTTGTTGACATA GTTGACCAGCTTTTT; CTSL1 (2): CCGGCCAAAGACCGGAGA AACCATTCTCGAGAATGGTTTCTCCGGTCTTTGGTTTTT.

The siRNA sequences and the sequences of the quantitative PCR primers are published elsewhere (Rafn et al., 2012). PCR primers were from TAG Copenhagen and siRNAs were purchased within the Sigma−Aldrich Functional Genomics Partnership Program. Except to this were the siRNAs for JAK1, JAK2 and JAK3 which were purchased from Life Technologies. The following previously unpublished (Rafn et al., 2012) qPCR primers were used: JAK1 forward; TCTGTTTGCTCAGGGACAGT and JAK1 reverse; AGCCATCCCTAGACACTCGT; JAK2 forward; TGCCGGTATGACCCTCTACA and JAK2 reverse; TAGAT TACGCCGACCAGCAC; JAK3 forward; ATTTTCTGGTATGCCCC CGA and JAK3 reverse; TCACATCCCATCATCCGCAG.

2.2. Tissue culture

MCF7 p95ΔN-ErbB2 cells or corresponding empty vector cells were established and cultured as described previously (Egeblad et al., 2001; Rafn et al., 2012). Expression of p95ΔN-ErbB2 was induced by washing of tetracycline with PBS. The vector control cells were treated the same way. Induced cells were cultured in RPMI 1640 Glutamax™ medium supplemented with 6% FBS and 0.25% penicillin and streptomycin. All experiments were carried out in passage three or four after induction. SK-OV3 (ATCC) cells were cultured in RPMI 1640 Glutamax™ medium supplemented with 10% FBS and 0.25% penicillin and streptomycin. SK-OV3.ip1 cells were established as described previously (Yu et al., 1993) and cultured in DMEM (GIBCO™, Invitrogen) supplemented with 10% FBS and 0.25% penicillin and streptomycin. HEK293 cells were cultured in DMEM supplemented with 10% FBS, 0.25% penicillin and streptomycin and 1% NEAA (GIBCO™, Invitrogen).

NALM-6 cells were cultured in RPMI 1640 Glutamax™ medium supplemented with 10% FBS and 0.25% penicillin and streptomycin.

2.3. Lentiviral-mediated gene knockdown

Lentiviral particles were produced in HEK293 cells using psPAX2, a packaging vector containing the minimal set of lentiviral genes required to generate the virion structural proteins and packaging functions, PMD2.G, a vesicular stromatitis virus G-protein envelope vector that provides the heterologous envelope for pseudotyping and pLK0.1, a shRNA transfer vector (Sigma−Aldrich). The specific shRNAs were from Sigma−Aldrich. HEK293 cells were seeded in 9 cm petri dishes (NUNC, Thermo Scientific) 24 h prior to transfection. Transfections were performed with Fugene HD (Roche Diagnostics) according to manufacturer's protocol using 2 μg of each vector. Cells were incubated overnight in the P2 laboratory and the culture medium was changed less then 24 h after transfection. Lentiviral particles were precipitated 48 h after transfection using Lentiviral Vector PEG-it™ Precipitation Kit (System Biosciences) according to manufacturer's protocol. For viral infection, the viral particles were added to the cell medium 24 h after seeding. All shRNA expressing cell lines were maintained and analyzed as pools and no single cell cloning was performed.

2.4. Transfections

siRNA transfections were done in 96-well plates with Oligofectamine (Invitrogen) utilizing reverse transfection with 60 nM siRNA concentration according to manufacturer's protocol. Transfections performed in 6-well plates were done using RNAiMAX (Life Technologies) with 25 nM siRNA concentrations.

2.5. Inhibitor treatments

Cells were seeded to 6-well plates 24 h prior to treatment with pharmacological inhibitors. For 48 h treatments, new inhibitor-dilutions were prepared after 24 h and the media was replaced. All inhibitor stocks were diluted in DMSO.

2.6. Cysteine cathepsin activity measurement

Cysteine cathepsin zFRase activity was measured as described previously (Dietrich et al., 2004).

2.7. Cell death assay-propidium iodide staining

Cells were seeded in 6-well plates 24 h prior treatment with pharmacological inhibitors. After treatment for 24 h, the cells were stained for 10 min in the dark with Hoechst-33342 (1:10000) (Invitrogen) and propidium iodide solution (1:5000) (Sigma−Aldrich) diluted in HEPES buffer (10 mM HEPES pH 7.4, 140 mM NaCl, 5 mM $CaCl_2$) to determine total cell count and cell death count, respectively. Cell death count and total count were determined using the Celigo Cytometer (Brooks Life Science Systems) and data were analyzed using Celigo Software Version 2.1. Hoechst-33342: Excitation 350, Emission 461. Propidium iodide: Excitation 535, Emission 617.

2.8. Cell death assay-lactate dehydrogenase (LDH) cytotoxicity measurement

LDH assay was carried out and the LDH activity was measured according to manufacturers instructions (Roche).

2.9. Immunoblotting

Cells were harvested and lysed using TR3 lysis buffer (3% SDS, 10% glycerol, 10 mM Na_2HPO_4) and sonicated on a Bioruptor™ (Diagenode). Protein concentrations were measured using the Thermo Scientific NanoDrop 2000 Spectrophotometer (Biocompare™, Thermo Scientific) and the lysate volume was adjusted accordingly to ensure equal loading. For detection of phosphor-ErbB2 and phosphor-Stat3, cells were harvested and lysed on ice using RIPA lysis buffer (1×PBS, 1% NP-40, 0.5% sodium deoxycholate, 0.1% SDS) supplemented with protease inhibitors (Complete Mini, Roche) and phosphatase inhibitors (Phosphatase Inhibitor Cocktail, Active Motif). Lysates were centrifuged at 10,000 × g for 10 min at 4 °C to obtain the total cell lysate and sonicated (Bioruptor™, Diagenode). Protein concentrations were measured by BCA™ protein assay (Pierce, Thermo Scientific) according to manufacturers protocol and lysate concentration was adjusted thereafter to ensure equal loading. Pre-boiled 4×LSB were added to lysate samples to reach a final concentration of 1×. All protein lysates were boiled for 5 min and then separated by SDS-PAGE using precast 4—15% gradient gels (BioRad). Gels were transferred to nitrocellulose membrane (BioRad) using Trans-Blot Turbo™ Transfer System and blocked in 5% milk. Novex™ Sharp Protein Standard (Invitrogen) was used to evaluate molecular weights of proteins from the gels. Primary antibodies were diluted in 5% BSA and incubated overnight at 4 °C on a rocking device. Horseradish peroxidase (HRP) conjugated secondary antibodies were diluted in 5% milk and incubated for 1 h at room temperature. The immunoblots were developed using Amersham™ ECL (GE Healthcare), and pictures were acquired by the luminescent image analyzer LAS-4000 mini (Fujifilm, GE Healthcare).

2.10. Real-time PCR analysis

Total RNA was isolated using Nucleospin™ Total RNA Isolation Kit (Macherey-Nagel) according to kit protocol. Complementary DNA was synthesized from 1 μg RNA using TaqMan™ Reverse transcription Kit (Roche Diagnostics) following manufacturer's protocol. Reverse transcription was performed on a Gradient Thermocycler (Biometra). Real-time PCR (RT-PCR) analysis was performed with FastStartPLUS SYBR Green 1 Mastermix (Roche Diagnostics) or SYBR Green QPCR Master Mix (Agilent Technologies) on a LightCycler 2.0 (Roche Diagnostics) or a 7500 Fast Real-Time PCR System (Applied Biosystems), using 0.4 μM primer concentration (TAG Copenhagen) according to manufacturer's protocol. Expression levels of target genes were normalized to expression levels of the housekeeping gene *PPIB*. The Pfaffl method (Pfaffl, 2001) was used to calculate relative mRNA levels.

2.11. 3D Matrigel invasion assay

Cells were grown on a lid of a 90 mm tissue culture dish overnight in a hanging drop containing 6.5×10^4 cells in 18 μL DMEM or RPMI (GIBCO™) supplemented with 10% FBS and 0.25% penicillin and streptomycin to establish multicellular spheroids. The following day, cell spheroids were transferred to a layer of 16 μL polymerized Matrigel (growth factor reduced; Becton Dickenson) diluted 1:1 with medium with or without 2× concentration of indicated inhibitor. Cell spheroids were covered with a sealing layer of 10 μL of Matrigel and then with complete medium supplemented with inhibitors or not as indicated in the text and in the figures. For 48 h inhibitor treatments fresh medium with inhibitors were added after the first 24 h. Cells spheroids were grown in 3D cultures and extend of invading growth were followed up to 3 days. Images were taken with Olympus 1×71 light microscope using the Cella P software. Quantification of data was done using MultiGauge Fuji Film. Cell sphere boundaries were defined and the average extend of invading outgrowth for all spheroids were measured.

2.12. Immunohistochemistry

Sections for each treatment were either subjected to hematoxylin and eosin (HE) staining or immunostained for proliferating cell nuclear antigen (PCNA) or activated Bax. For HE staining, sections were deparafinized in TissueTeck (Sakura), hydrated in graded ethanol, stained for hematoxylin and eosin and finally dehydrated in graded ethanol. After drying at room temperature, sections were mounted with Pertex (HistoLab Products AB) and the stainings were visualized with Leitz Laborlux light microscope. For antibody staining, sections were deparafinized in TissueTeck (for PCNA) or xylene (for Bax), covered with 99% ethanol, covered with blocking peroxidase solution (12% H_2O_2 in 99% ethanol) for 15 min and then rinsed in 96% and 70% ethanol. Sections were then subjected to protein retrieval by boiling them in 0.01 M Na citrate buffer (0.01 M Na citrate; for PCNA) or TE buffer (10 mM Tris—HCl pH8, 0.1 mM EDTA; for Bax) for 10 min. After cooling, sections were rinsed in TBS (50 mM Tris—HCl ph 7.4, 150 mM NaCl) with 1% FBS. Primary antibody, diluted 1:600 (PCNA) or 1:1000 (Bax) in TBS with either 1% (Bax) or 10% (PCNA) FBS, was added and left for incubation for 1 h in a humidified chamber. Following wash in TBS, sections were incubated with secondary anti-mouse EnVision (DAKO) for 30—45 min and then washed with TBS. Color was developed by incubating with enhanced DAB (DAKO). Section were dehydrated in graded ethanol, dried and mounted with Pertex. Stainings were visualized with Leitz Laborlux light microscope or Olympus Model 1×71S8F-3 light microscope. With regard to the activated Bax staining, the images were quantified in respect to activated Bax using ACIS III Chromavision Systems and ACIS III software (DAKO). 5—10 independent 20× regions were placed at the boarder of each cell sphere, 2—4 cell spheres per treatment. The percentage of brown stained area (activated Bax) of the total stained area was determined.

2.13. Immunofluorescence microscopy

Cells were seeded on glass coverslips in 24-well plates (NUNC, Thermo Scientific). For inhibitor treatment, cells were treated 24 h after seeding and fixed 24 h after the treatment. For siRNA treatment, cells were transfected and then reseeded on coverslips the next day and fixed 72 h later. For fixation, cells were washed twice with PBS, incubated for 15 min with 3.7% formaldehyde at room temperature, incubated with methanol for 3 min at −20 °C, and finally washed twice with PBS. Cells were covered with blocking buffer (PBS with 1% BSA, 0.3% Triton-x 100) supplemented with 5% universal goat serum (DAKO) for minimum 20 min at room temperature. Primary antibodies, diluted in blocking buffer without serum, was added and left for incubation for 1–2 h at room temperature, followed by wash with wash buffer (PBS with 0.25% BSA,

0.1% Triton-x 100). Secondary antibodies, diluted in wash buffer supplemented with 5% universal goat serum, were added and left for incubation for 1 h at room temperature. Slips were washed once with PBS plus 0.05% Tween, once in PBS plus 0.05% Tween plus Hoechst (50 μg), and once with PBS plus 0.05% Tween. Finally the slips were washed with MilliQ water and then mounted with preheated ProLong Anti-fade Gold Mounting Medium (Invitrogen), which was left to solidify overnight at room temperature. Images were taking with a LSM510 Meta microscope (Carl Zeiss, Inc). Quantification of lysosomal distribution was done by classifying cells into perinuclear-dominant lysosomal pattern (more than 50% of the LAMP-2 stained vesicles localized in the perinuclear region), and peripheral-dominant pattern (more than 50% of the LAMP-2 stained vesicles localized in the peripheral region), and uniform dispersed lysosomal pattern (more than
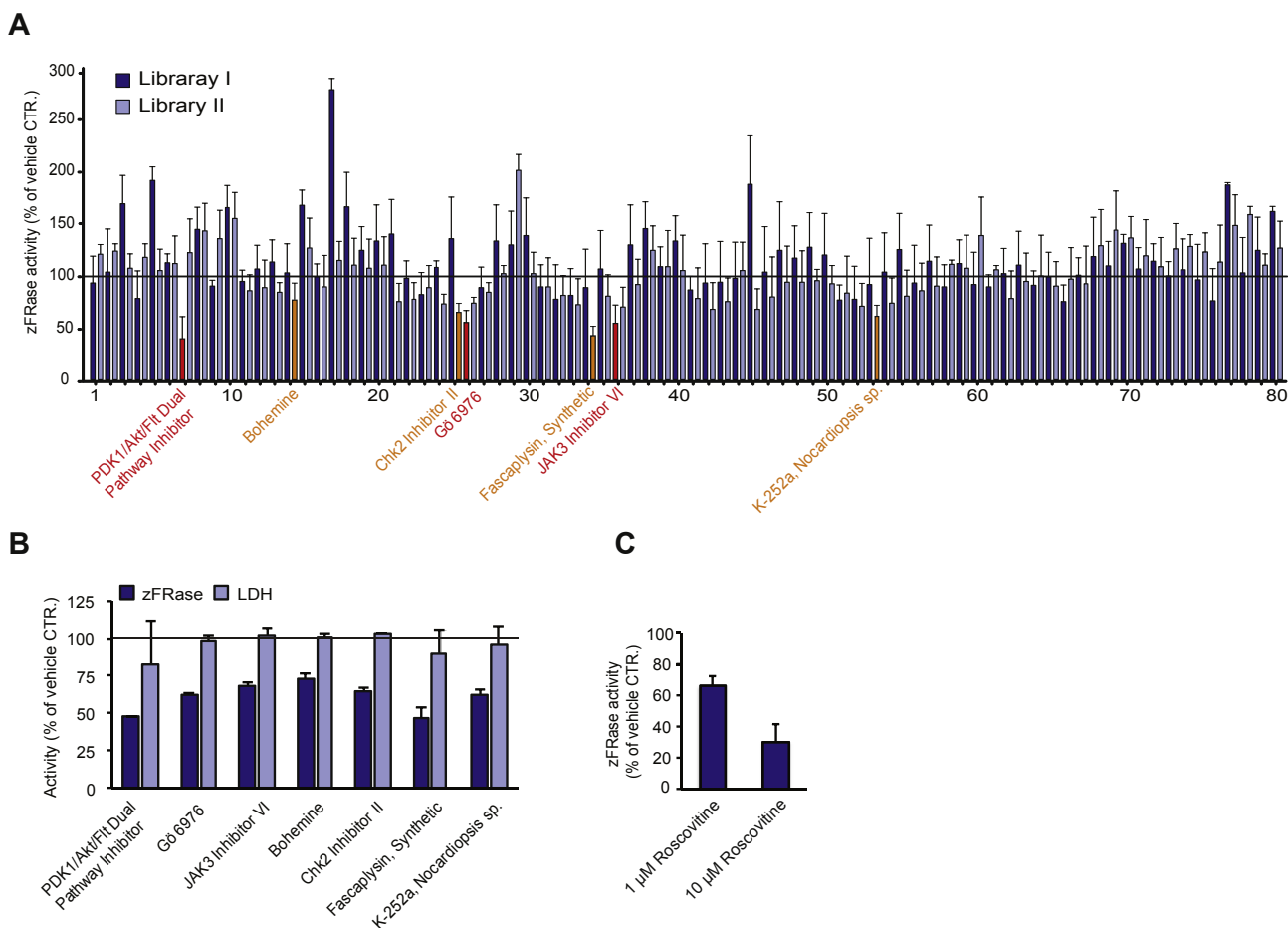

Figure 1 — A pharmacological kinase inhibitor screen identified compounds that decrease cysteine cathepsin activity. (A) Inhibitor screen. MCF7 p95ΔN-ErbB2 cells were seeded in 96-well plates 24 h prior inhibitor-treatment. Cells were treated with 1 μM kinase inhibitor from Inhibitor Select Libraries I (dark blue and red) and II (light blue and orange) (Calbiochem) for 24 h. DMSO was used as a vehicle control. zFRase activity was normalized to protein concentration. Best screening hits from the inhibitor Select Libraries I and II are marked with red and orange, respectively. Mean ± Stdev are based on three independent screens. (B) zFRase activity and lactate dehydrogenase (LDH) activity measurements for p95ΔN-ErbB2 MCF7cells. Cells were treated with 1 μM of the indicated kinase inhibitors collected from the Inhibitor Select Libraries I and II (Calbiochem) for 24 h. DMSO was used as a vehicle control. zFRase activity and LDH activity was normalized to protein concentration. Mean ± Stdev for zFRase activity are based on three independent experiments. Mean ± Stdev for LDH activity represent standard deviation from the mean of triplicates from one experiment. (C) zFRase activity measurement of MCF7 p95ΔN-ErbB2 cells treated with 1 μM or 10 μM Roscovitine for 24 h zFRase activity was normalized to protein concentration. Data are representative of three independent assays. Mean ± Stdev represent standard deviation from the mean of triplicates from one experiment.

50% of the LAMP-2 stained vesicles localized neither in the perinuclear nor the peripheral region). Quantification is based on at least three independent experiments, each carried out as duplicates, and 10—20 cells were counted on each image taken. The results are illustrated as percentage of predominant lysosomal distribution in the total number of cells assayed.

2.14. Statistical analysis

For Figure 5B and F the experiment was repeated at least three times and compared by unpaired two-tailed t-test to corresponding non-targeting control siRNA treated cells and vehicle control treated cells, respectively. The statistical significance is illustrated with p-values; *, p 0.05; **, p 0.01 and ***, p 0.001.
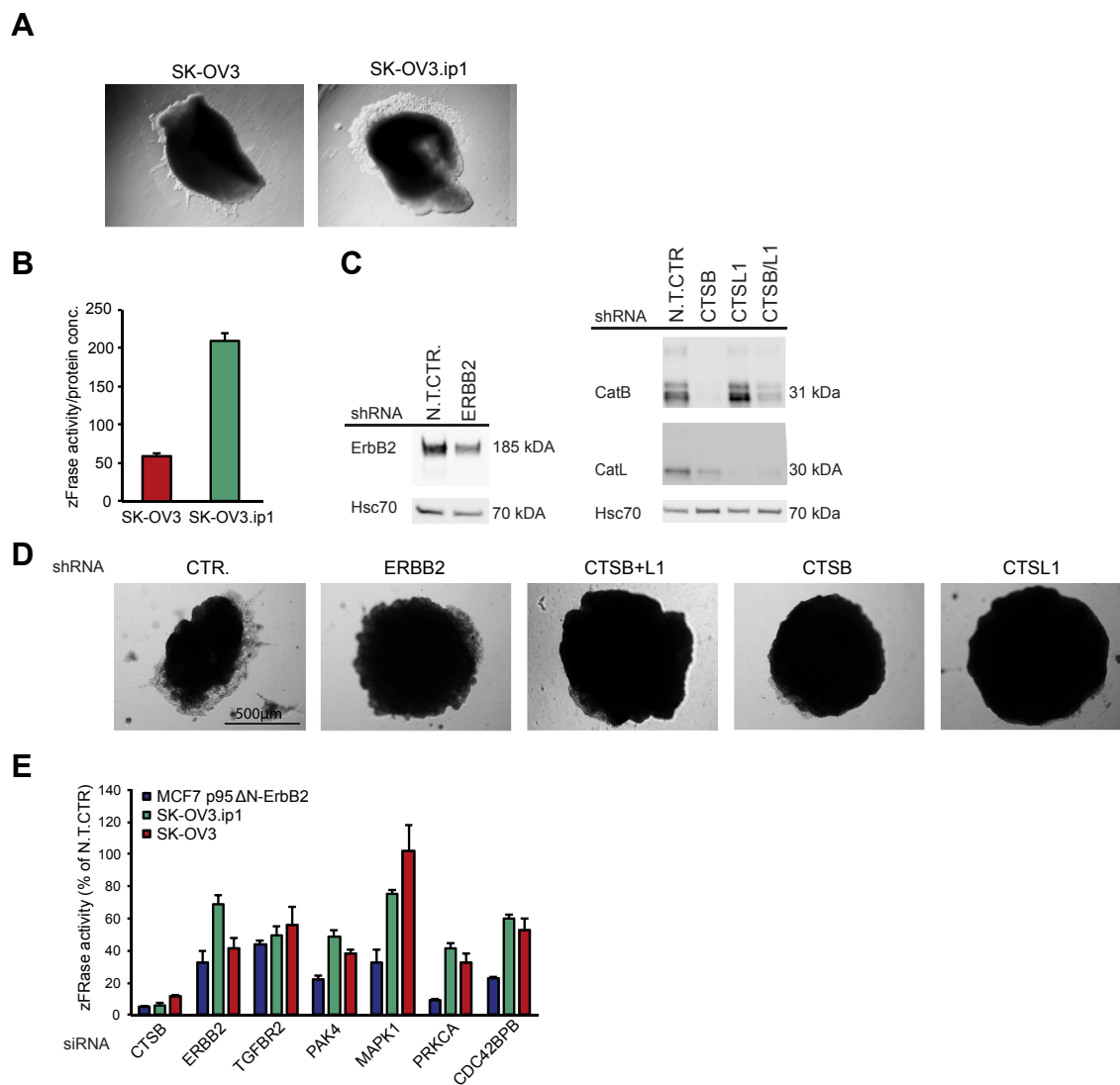

Figure 2 — ErbB2 drives invasiveness of ErbB2-positive ovarian cancer cell lines via a signaling network similar to that in ErbB2-positive breast cancer cells. (A) 3D Matrigel invasion assay. SK-OV3 and SK-OV3.ip1 cells were grown in hanging drops overnight to establish multicellular spheroids. Cell spheroids were grown inside thin-layered Matrigel clumps for up to 72 h and visualized with Olympus 1×71 light microscope for detection of invading growth. Images are taken with 10× magnification. Images shown are representative of each cell line. (B) zFRase activity measurement for SK-OV3 and SK-OV3.ip1 cells. zFRase activity was normalized to protein concentration. Data are representative of three independent experiments. Mean ± Stdev represent standard deviation from the mean of triplicates from one experiment. (C) Immunoblot analysis for the detection of ErbB2, cathepsin B and cathepsin L in SK-OV3.ip1 cells stably depleted of ErbB2, cathepsin B, cathepsin L and cathpsin B + L using shRNAs. Hsc70 was used to control equal loading. (D) 3D Matrigel invasion assay. SK-OV3.ip1 control cells and SK-OV3.ip1 cells stably depleted of ErbB2, cathepsin B, cathepsin L and cathepsin B + L were grown in hanging drops overnight to establish multicellular spheroids. Cell spheroids were grown inside thin-layered Matrigel clumps for up to 72 h and visualized with Olympus 1×71 light microscope for detection of invading growth. Images are taken with 10× magnification. The scale bar represents 500 μm. Images shown are representative of the indicated cell line. (E) zFRase activity of p95ΔN-ErbB2 MCF7, SK-OV3.ip1 and SK-OV3 cells treated with 60 nM of the indicated siRNAs for 72 h zFRase activity was normalized to total protein concentration and is presented as the percentage of the activity in cells transfected with a non-targeted control siRNA (N.T.CTR.). Data are representative of three independent experiments. Mean ± Stdev represent standard deviation from the mean of triplicates from one experiment.

3.   Results

3.1.   Identification of novel compounds that inhibit ErbB2-induced cysteine cathepsin activity

ErbB2-induced lysosomal cysteine cathepsin activity (zFRase activity) is needed for the invasion of MCF7 cells expressing an inducible, constitutively active 95 kDa NH$_2$-terminally truncated p95 form of ErbB2 (p95ΔN-ErbB2) as well as of ErbB2-positive SK-BR-3 and MDA-MB-453 breast cancer cells (Rafn et al., 2012). Here we set up a small-scale screen to find out, if drug-induced decrease in the cysteine cathepsin

activity (zFRase activity) could be used as a tool to identify novel inhibitors of ErbB2-induced, cysteine cathepsin mediated invasion. As inhibitor source we used the InhibitorSelect kinase inhibitor libraries I and II (Calbiochem, Supplementary Table I). Although these libraries are relatively small, we expected to find compounds that can decrease zFRase activity, since we had previously identified several kinases as mediators of ErbB2-induced, cysteine cathepsin mediated invasion (Rafn et al., 2012). Moreover, poor specificity of many kinase inhibitors (Bain et al., 2007) can further increase chances to find suitable compounds. We seeded the MCF7 p95ΔN-ErbB2 cells (Egeblad et al., 2001; Rafn et al., 2012) into 96-well plates so that they reached 80% confluence 24 h later, when we
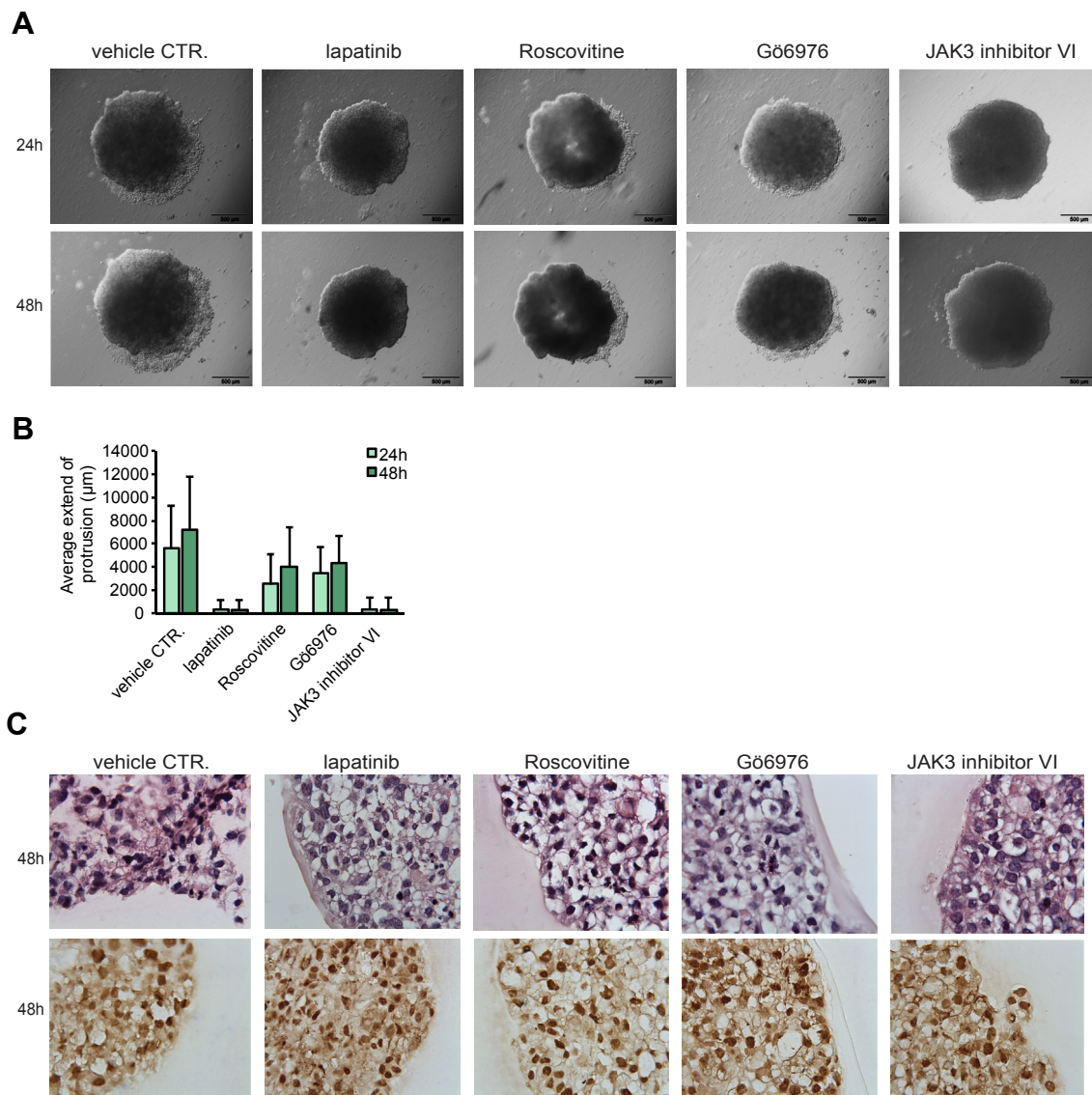

Figure 3 − Lapatinib and JAK3 inhibitor VI completely inhibit cell invasion. (A) 3D Matrigel invasion assay. SK-OV3.ip1 cells were grown in hanging drops overnight to establish multicellular spheroids. Cell spheroids were grown inside thin-layered Matrigel clumps for 24 h after treatment with 10 μM final concentration of the indicated inhibitors. After 24 and 48 h the spheroids were visualized with Olympus 1×71 light microscope to detect invading growth. Images are taken with 6,4× magnification and the scale bar represents 800 μm. Images shown are representative of each treatment. (B) Quantification of invasive growth. (C) Hematoxylin-eosin and proliferating cell nuclear antigen (PCNA) antibody staining of sections made from the samples of (3A). Matrigel-embedded cell spheroids were fixed in paraffin and sections were prepared. Sections for each treatment were either subjected to hematoxylin-eosin (top) staining or stained for PCNA (bottom). Images are taken with 40× magnification and are representative of each treatment.
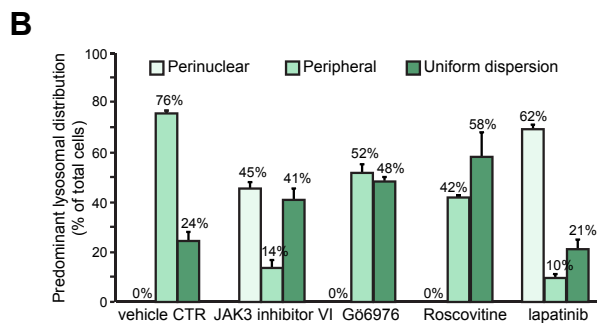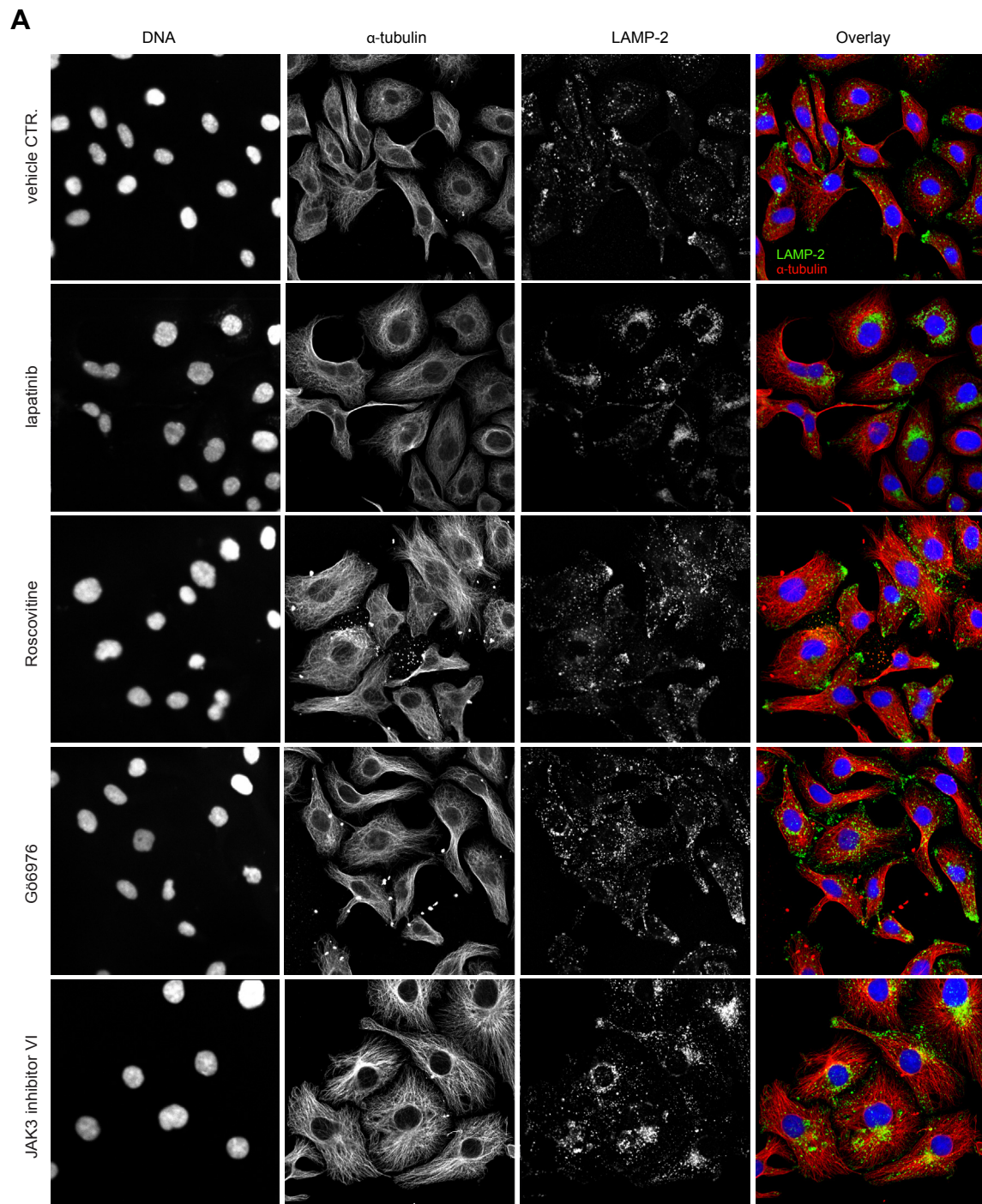
A

B

Figure 4 − Lapatinib and JAK3 inhibitor VI treatments change lysosomal distribution from the cell periphery to the perinuclear area. (A) Confocal immunofluorescence images for the detection of lysosomal membrane protein 2 (LAMP-2) for lysosome localization. SK-OV3.ip1 cells were

treated them with 1 μM library inhibitors or DMSO vechile control for additional 24 h. The procedure was carried out trice. Seven compounds were repeatedly found to substantially decrease the zFRase activity (Figure 1A). The 24 h timepoint and low concentration was chosen to avoid induction of cell death. These conditions were suitable for all the compounds identified, since all of them could decrease zFRase activity without inducing cell death (Figure 1B). We selected some of the compounds for further studies. We chose Gö6976 and JAK3 inhibitor VI, because both were recently identified as potent inhibitors of autophagy (Farkas et al., 2011), a process involving lysosomes. We additionally chose Bohemine, a cyclin dependent kinase inhibitor that, among others, inhibits ERK8 and PAK4 (Bain et al., 2007) and who's derivative Roscovitine (also known as Selicilib) is currently in clinical trial as a combinatory anti-cancer agent to treat advanced solid tumors. Especially, Roscovitine possesses tumor suppressive activity on therapy-resistant breast cancer cells (Nair et al., 2011). Because Roscovitine was also efficient in decreasing zFRase activity (Figure 1C), we replaced Bohemine with Roscovitine for the rest of the studies.

3.2. Setting up an invasion assay for ErbB2 expressing ovarian cancer spheroids

Since the screen was done with cells that express p95 ErbB2, we decided to set up a model system with high endogenous expression of full-length p185 ErbB2 to find out if the identified compounds also inhibit their ErbB2-induced, cathepsin mediated invasiveness. We used SK-OV3 ovarian cancer cell line (HER2 3[+]) and its subline SK-OV3.ip1 that has been established earlier by intraperitoneal passage of SK-OV3 cells and found to be more aggressive than the parental cell line, most likely due to its enhanced ErbB2 activity (Yu et al., 1993). We subjected them to 3D Matrigel invasion assay and found SK-OV3.ip1 cells to be even more invasive than SK-OV3 (Figure 2A). zFRase activity assay revealed that SK-OV3.ip1 had higher cysteine cathepsin activity (Figure 2B). We made stable cell lines of SK-OV3 using three different shRNAs for ERBB2 and two different for both CTSB and CTSL1 (Supplemental Figure 1A). Of these we chose the ones with the most efficient target depletion for 3D Matrigel invasion assays. We found the depletion of ERBB2, CTSB, CTSL1 and CTSB + L1 efficiently inhibiting invasion of these cells (Supplemental Figure 1B). We next chose the most efficient shRNAs for each of the mRNAs to downregulate them in SK-OV3.ip1 cells (Figure 2C). As the invasion of MCF7 p95ΔN-ErbB2 cells (Rafn et al., 2012) and the parental SK-OV3 cells (Supplemental Figure 1B), the invasion of the SK-OV3.ip1 cells was dependent on ErbB2, cathepsin B and cathepsin L (Figure 2D). Both SK-OV3 and SK-OV3.ip1 were found to invade faster than the MCF7 p95ΔN-ErbB2 cells, SK-OV3.ip1 being the most aggressive ErbB2 expressing cancer cells we have identified thus far. The kinases that were identified to mediate the ErbB2-induced zFRase activity and invasiveness in MCF7 p95ΔN-

ErbB2 cells (Rafn et al., 2012) also regulated the zFRase activity of the SK-OV3 and SK-OV3.ip1 cells as efficiently as the MCF7 p95ΔN-ErbB2 cells with the exception of ERK2 (Figure 2E). In this assay the siRNA-based depletion of kinases was efficient (Supplemental Figure 1C). Thus, we had established a novel 3D invasion model system where invasiveness in 3D Matrigel is driven by ErbB2 and mediated by cathepsins B and L. Importantly; we had also established a central role for ErbB2 signaling-induced cysteine cathepsin activity in the invasion of ErbB2-positive ovarian cancer cells.

3.3. All identified compounds can inhibit invasion in 3D assays but with varying efficiency

We further analyzed Roscovitine, Gö6976 and JAK3 inhibitor VI using the highly invasive SK-OV3.ip1 cell line and the ErbB2 inhibitor lapatinib as a positive control. Lapatinib is a fluorescence compound interfering with the zFRase assay and thus it could not be used in the assay. We instead used lapatinib to control the 3D invasion assay. We mixed the inhibitors at 10 μM concentration with the Matrigel. We transferred the overnight "hanging drop" cultured SK-OV3.ip1 spheroids inside Matrigel clumps and immersed the clumps into cell culture media containing 10 μM final concentration of the indicated inhibitors or DMSO vehicle control. We followed the cells inside the 3D Matrigel clumps up to 48 h and quantified their invasion as described before (Rafn et al., 2012) (Figure 3A). Already after 24 h lapatinib almost completely inhibited invasion of SK-OV3.ip1 cells (Figure 3A, B). Both Roscovitine and Gö6976 treatments had measurable inhibitory effect when compared to the DMSO vehicle control treated cells (Figure 3A, B). Interestingly, treatment with the JAK3 inhibitor VI inhibited invasion as efficiently as lapatinib (Figure 3A, B). We fixed the spheres and stained with an antibody against proliferating cell nuclear antigen (PCNA) and found the inhibitor treated cells alive and proliferating inside the Matrigel still at the 48 h time point (Figure 3C). 24 h treatment of SK-OV3.ip1 cells with 1 μM and 10 μM inhibitors did not induce cell death over the basal level as measured by propidium iodide staining (Supplemental Figure 2A). We also stained the spheres from Figure 3A at 48 h time point with antibody recognizing Bax activation (Ellegaard et al., 2013), a sign of activated apoptosis, and found less than 1% of cells (except for Roscovitine) harboring activated Bax (Supplemental Figure 2B). These results demonstrate that lapatinib as well as Gö6976, Roscovitine and JAK3 inhibitor VI can inhibit invasiveness of the ErbB2-positive, highly invasive SK-OV3.ip1 cells in 3D Matrigel cultures.

3.4. Lapatinib and identified compounds reverse ErbB2-induced malignant lysosomal distribution

Prompted by previous work showing that inhibition of the ErbB2-induced zFRase activity can reverse the ErbB2-induced localization of lysosomes to the invasive protrusions at the

treated with 10 μM of the indicated inhibitors for 24 h after which they were fixed and stained for the detection of the lysosomal membrane protein LAMP-2 (green), alpha tubulin (red) and nucleus (blue). Images shown are representative of each treatment from three independent experiments. (B) Quantification of predominant lysosomal distribution from cells on images in (4A).
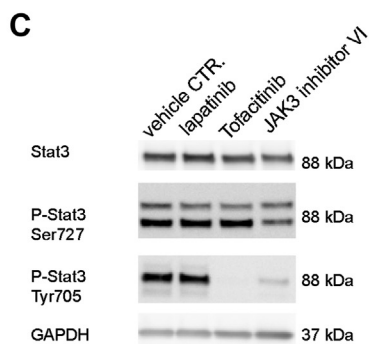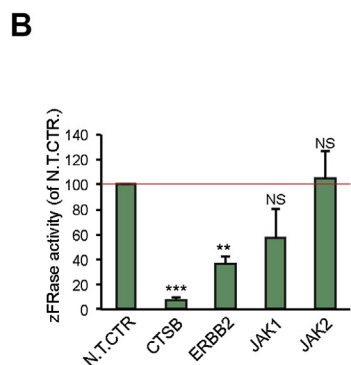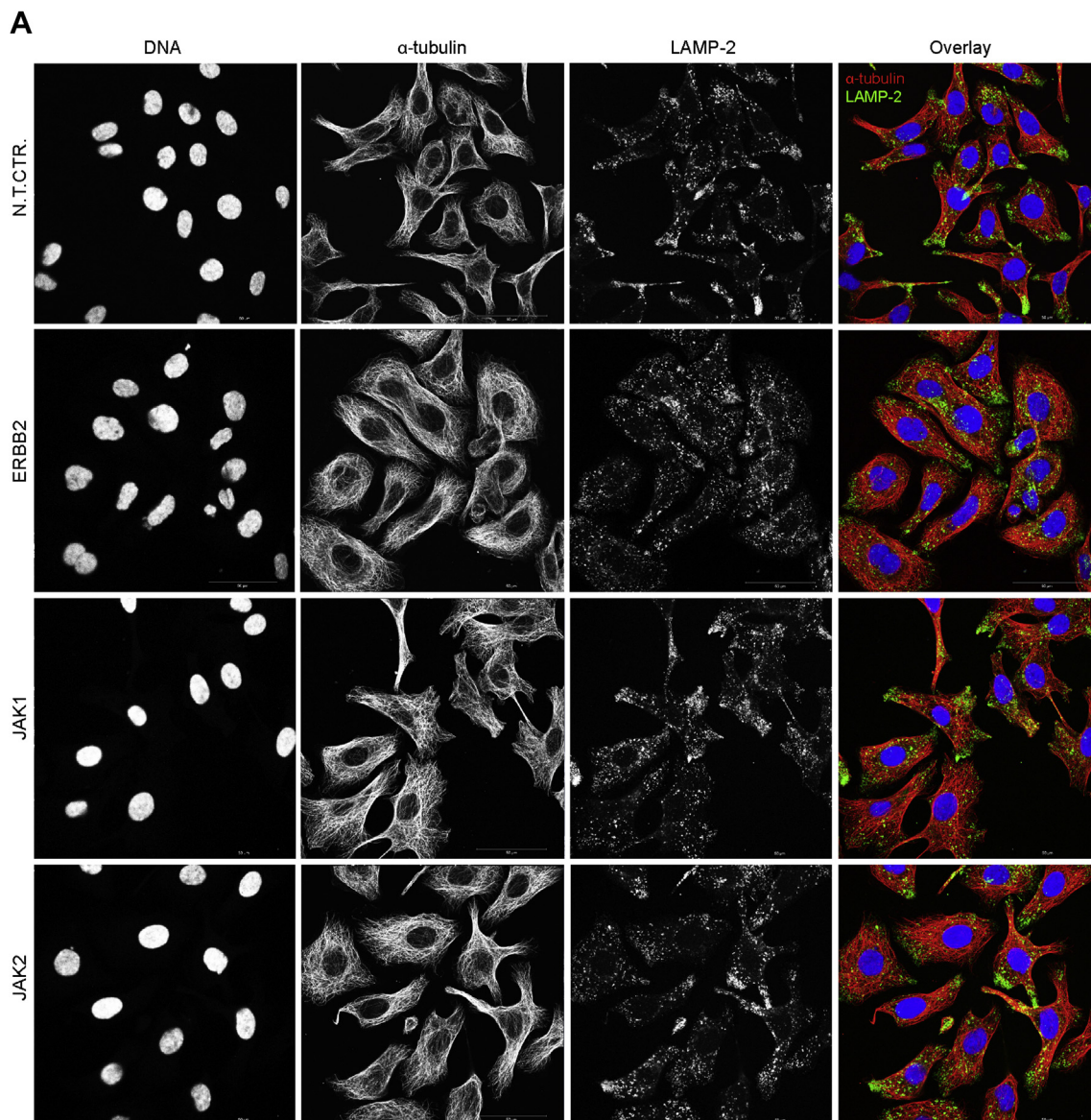
Figure 5 − JAK3 inhibitor VI treatment inhibits invasion of ErbB2-positive cells with a mechanism that is independent of JAKs but involves ErbB2 and CTSL1 downregulation. (A) Confocal immunofluorescence images for the detection of LAMP-2 localization. SK-OV3.ip1 cells were treated with 25 nM of the indicated siRNAs for 96 h after which they were fixed and stained for the detection of the lysosomal membrane protein LAMP-2 (green), alpha tubulin (red) and nucleus (blue). Images shown are representative of each treatment from three independent experiments. (B) zFRase activity of SK-OV3.ip1 cells treated with 25 nM of the indicated siRNAs for 96 h zFRase activity was normalized to total protein concentration and is presented as the percentage of the activity in cells transfected with a non-targeted control siRNA (N.T.CTR.). Mean ± Stdev represent standard deviation from the mean of three independent experiments. (C) Immunoblot analysis of inhibitor treated cells. SK-OV3.ip1 cells were treated with 10 μM of the indicated inhibitors for 24 h. STAT3 was used to control the phosphor-STAT3 blot and GAPDH was used to
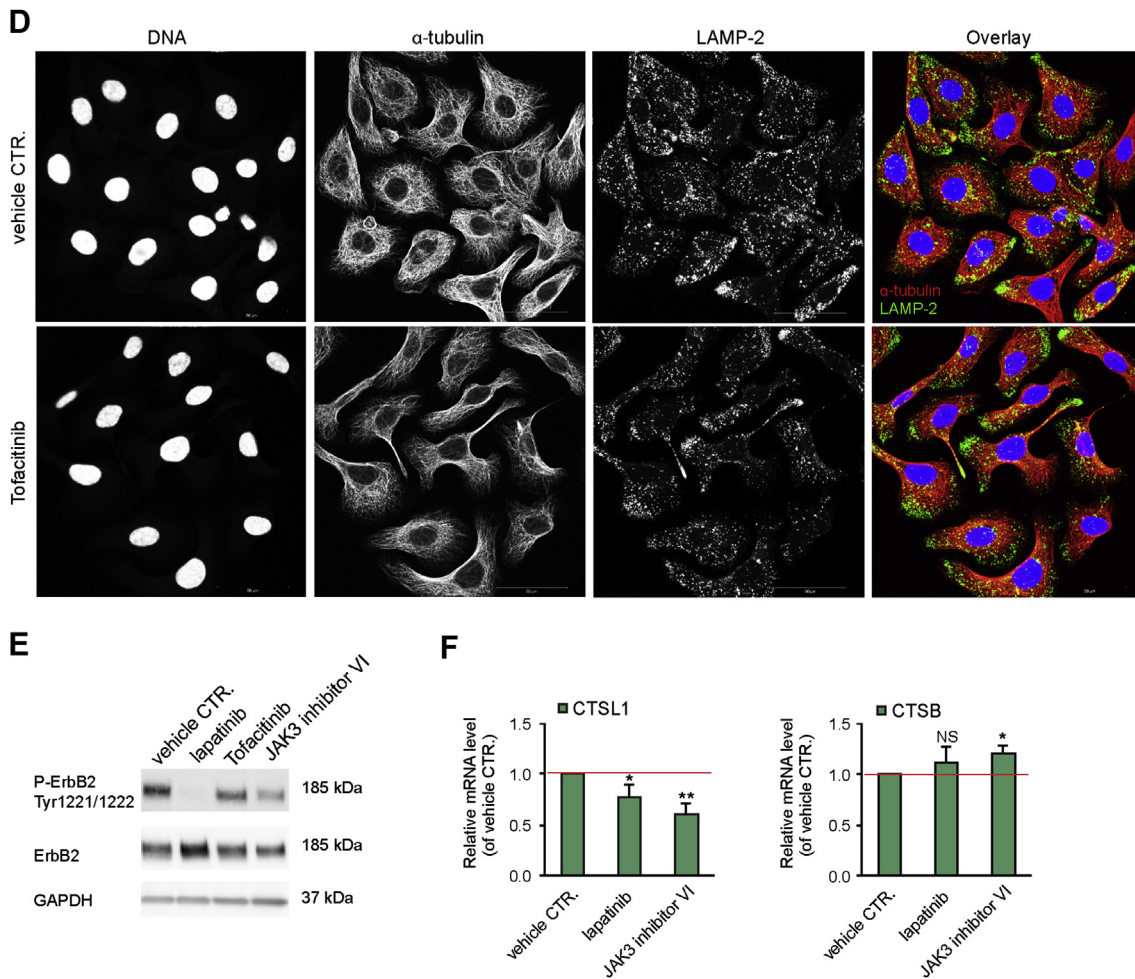
Figure 5 — *(continued)*

cell periphery (Rafn et al., 2012), we treated the SK-OV3.ip1 cells with 10 μM of inhibitors or vehicle control for 24 h, fixed them and used the confocal microscopy and staining of the lysosomal membrane protein 2 (LAMP-2; green) to detect the lysosomes, α-tubulin to visualize the cytoskeleton (red) and Hoechst for the nucleus (blue) (Figure 4A). Both lapatinib and JAK3 inhibitor VI could efficiently inhibit the ErbB2-mediated pericellular distribution of lysosomes (Figure 4A, B). A similar effect, however milder, was observed with Roscovitine and Gö6976 treatments (Figure 4A, B). Thus, all of these drugs affected lysosomal distribution and made lysosomes migrate from their oncogenic and invasion-promoting, pericellular position into a perinuclear position, where their secretion and exocytosis into the extracellular space gets less likely.

3.5. Analysis of the potential mechanism involved in JAK3 inhibitor VI-mediated invasion inhibition

Since JAK3 inhibitor VI was found to be the most efficient, novel invasion inhibitor matching lapatinib with its potency, we investigated its function more closely. Immunoblot analysis indicated that SK-OV3.ip1 cells were not expressing JAK3 (Supplemental Figure 3A). Since JAK3 inhibitor VI can also efficiently inhibit JAK1 and JAK2 (Anastassiadis et al., 2011), we depleted JAK1 and JAK2 from SK-OV3.ip1 cells (Supplemental Figure 3B) and studied its effect on lysosomal distribution (Figure 5A) and zFRase activity using *CTSB* and *ERBB2* siRNAs as positive controls (Figure 5B). These studies showed that either JAK1 or JAK2 depletion had no effect on

control equal loading. The blots shown are representatives of more than three independent experiments. **(D)** Confocal immunofluorescence images for the detection of LAMP-2 lysosome localization. SK-OV3.ip1 cells were treated with 10 μM of the indicated inhibitors for 24 h after which they were fixed and stained for the detection of the lysosomal membrane protein LAMP-2 (green), alpha tubulin (red) and nucleus (blue). Images shown are representative of each treatment from three independent experiments. **(E)** Immunoblot analysis of inhibitor treated cells. SK-OV3.ip1 cells were treated with 10 μM of indicated inhibitors for 24 h ErbB2 was used to control the phosphor-ErbB2 blot and GAPDH was used to control equal loading. The blots shown are representative of three independent experiments. **(F)** Quantitative RT PCR analysis for the detection of *CTSL1* and *CTSB* expression in SK-OV3.ip1 cells treated with 10 μM of the indicated inhibitors for 24 h. The mRNA expression was normalized to the expression of *PPIB*. Mean ± Stdev represent standard deviation from the mean of three or more independent experiments.

lysosome distribution and that only JAK1 depletion had a slight but insignificant inhibitory effect on the zFRase activity (Figure 5B). To further confirm that JAK inhibition was not involved, we used the JAK3 inhibitor Tofacitinib (CP690550), which is a rather specific JAK1, 2 and 3 inhibitor (Anastassiadis et al., 2011) and currently used the in the clinics for a treatment of rheumatoid arthritis in the United States. Treatment of cells with Tofacitinib, which efficiently inhibited STAT3 phosphorylation (Figure 5C), did not have any effect on lysosomal distribution (Figure 5D).

As evident from immunoblots, lapatinib treatment strongly decreased the ErbB2 phosphorylation, as was expected (Figure 5E). Interestingly, JAK3 inhibitor VI treatment decreased levels of both total ErbB2 and phosphorylated ErbB2 (Figure 5E). Similar to JAK3 inhibitor VI treatment, treatment of cells with Gö6976, which is a known PKCα inhibitor, decreased the levels of both ErbB2 and phosphor-ErbB2 (Supplemental Figure 3C). On the contrary to this, treatment of cells with Tofacitinib had no effect on ErbB2 level or phosphorylation (Figure 5E). Since cathepsins B and L are important for the ErbB2-induced invasion of SK-OV3.ip1 cells into Matrigel (Figure 2D), we studied if JAK3 inhibitor VI treatment can affect cathepsin B or L levels in these cells. Indeed, JAK3 inhibitor VI treatment decreased the CTSL1 level and did it even more efficiently than lapatinib (Figure 5F). However, treatment with neither of them decreased CTSB expression (Figure 5F). Since shRNA-based depletion of CTSL1 or CTSB efficiently blocked the invasion of SK-OV3.ip1 cells into Matrigel, it is likely that the JAK3 inhibitor VI-mediated decrease in the CTSL1 mRNA level contributes to the drug-induced, decreased invasion of the SK-OV3.ip1 cells. Thus, treatment of SK-OV3.ip1 cells with JAK3 inhibitor VI decreases their CTSL1 mRNA level significantly with a mechanism that most likely does not involve inhibition of any members of the JAK family but may involve impaired ErbB2 expression.

4.   Discussion

Here we present a simple screening system based on cysteine cathepsin activity and efficient follow-up assays for the identification of small cell-permeable inhibitor compounds that can inhibit invasion of aggressive and highly invasive ErbB2-positive cancer cells. In addition to ErbB2, other oncogenes such as Ras and Scr can increase cysteine cathepsin expression and activity. Increased cathepsin B and L activity is strongly linked to aggressiveness of various cancers for their virtue of positively contributing to invasion, angiogenesis and metastasis (Kallunki et al., 2013). Their invasion and metastasis promoting function is well documented in two mouse models of invasive cancer progression. In the first model, a pancreatic islet carcinogenesis model (Rip1-Tag2/RT2), the oncogenic SV40 T-antigen is expressed in insulin producing β-cells in mouse. This model shows that both cathepsin B and cathepsin L are important for tumor growth and invasion and that cathepsin B is additionally needed for tumor angiogenesis and that genetic inactivation of cathepsin B or cathepsin L strongly impairs tumor growth and invasion in vivo (Gocheva et al., 2006). Similarly, in the second model, mice which are established from cathepsin B knockout mice

that are crossed to mammary tumor virus−polyoma middle T antigen (PyMT) overexpressing mice, have significant delay in their mammary tumor formation and metastasis to lungs in comparison to cathepsin B wild type mice (Vasiljeva et al., 2006).

Variety of cathepsin B and L inhibitors has been developed with the idea of utilizing them as invasion inhibitors for different cancers. However, of cathepsin inhibitors thus far only odanacatib, an inhibitor of cathepsin K, a cathepsin with especially high osteolytic activity, is under clinical trial for treatment of osteoporosis-associated bone loss (Costa et al., 2011) and is proven promising against bone metastasizing breast cancer (Jensen et al., 2010). In drug-induced lysosomal membrane permeabilization lysosomal contents leaks into the cytosol and induces programmed cell death (Groth-Pedersen and Jaattela, 2013). Especially cathepsin B has been shown to be important in this process (Kirkegaard and Jaattela, 2009). Consequently in cancer, complete inhibition of cysteine cathepsin activity may interfere with drug-induced lysosomal cell death and result in poorer treatment responses. Thus, to inhibit invasion, a better lysosome-based strategy might be to inhibit cathepsin activity partially (e.g. the oncogene-induced activity that is needed for the invasion) or to inhibit lysosomal exocytosis and secretion of cathepsins to the extracellular space.

As for the p95 and full-length ErbB2 expressing breast cancer cells (Rafn et al., 2012), cathepsins B and L are also crucial for the in vitro invasiveness of the ErbB2-positive SK-OV3 and SK-OV3.ip1 ovarian cancer cells which express high amounts of full-length ErbB2. In addition of having higher ErbB2 expression and more enhanced ErbB2 downstream signaling than the parental SK-OV3 cells (Yu et al., 1993), the SK-OV3.ip1 cells also display increased expression of mesenchymal markers showing cancer stem cell like traits, which may contribute to their increased invasiveness (Strauss et al., 2011). Remarkably, lapatinib was able to completely inhibit the invasion of the SK-OV3.ip1 cells in 3D Matrigel invasion assays. Together with the corresponding ErbB2 shRNA experiments that gave similar results, this strongly suggests that ErbB2 is likely to be the main driver and responsible of the invasive potential of these ovarian cancer cells in 3D Matrigel cultures. On the other hand, expression of ErbB2 correlates positively with the stem cell marker ALDH in human primary breast cancer and overexpression of ErbB2 in various breast cancer cells facilitates mammosphere formation and invasion in vitro (Ginestier et al., 2007; Korkaya et al., 2008), suggesting for a potential link between ErbB2 expression and stemness of cancer cells.

Lapatinib is a potent and rather specific EGFR and ErbB2 inhibitor (Anastassiadis et al., 2011) that shuts down the EGFR and ErbB2 kinase activity thus inhibiting tumor growth, invasion and intravasation of ErbB2-positive cancer cells (Kedrin et al., 2009). In this study we describe a potentially important, novel function for lapatinib as a compound that can reverse the ErbB2-induced malignant, invasion-promoting pheripheral distribution of lysosomes. Translocation of lysosomes from their typical, mainly perinuclear position to the cellular periphery is a process that is involved in lysosomal exocytosis, whereby lysosomes migrate to the cell membrane, fuse with it and empty their contents to the extracellular space

(Settembre et al., 2013). Lysosomal exocytosis is an important cellular clearance mechanism strongly contributing to the well-being of cells and organisms. In normal, non-cancerous cells lysosomal exocytosis is transcriptionally tightly regulated by transcription factor EB (TFEB) (Settembre et al., 2013). Most cancer cells, including those overexpressing ErbB2, harbor constitutive activation of mTOR or ERK-MAPK signaling pathway, which leads to phosphorylation of TFEB at several serines and its nuclear exclusion making it uncabable of activating genetic programs that regulate lysosomal translocation and exocytosis (Pena-Llopis et al., 2011; Settembre et al., 2011). Cancer cells can utilize lysosomal exocytosis for invasion. It is currently not known how cancer cells activate lysosomal exocytosis. Not much is either known about its revese process whereby lysosomes return to their normal, non-secretory positions. Interestingly, lapatinib potently induced this process that is antagonistic to lysosomal exocytosis and coincides with the decrease of the invasive potential of the cells. This novel function of lapatinib may also contribute to its invasion and metastasis inhibiting function *in vivo*.

JAK3 inhibitor VI, the most efficient invasion inhibitor identified in this study, functions by directly binding to JAK3 and thereby preventing STAT5 phosphorylation (Adams et al., 2003). It can also efficiently inhibit JAK family members JAK1 and JAK2 (Anastassiadis et al., 2011). JAKs are involved in the cytokine-triggered signaling events mainly through tyrosine phosphorylation of the signal transducers and activators of transcription (STAT) proteins (Yamaoka et al., 2004). Several studies confirm a connection in ErbB2-induced invasion and STAT5 signaling in breast cancer (Nevalainen et al., 2004; Olayioye et al., 1999; Sultan et al., 2005; Ward et al., 2013). Of JAK family members especially JAK2 is interesting in respect to breast cancer, since it can promote activation of ErbB2, Src and Ras—MAP kinases (Liang et al., 2010; Ren and Schaefer, 2002; Yamauchi et al., 2000). Despite the evidenced cross talk between JAKs—STATs and ErbB2, our work suggests that the effect of JAK3 inhibitor VI on the ErbB2-induced cysteine cathepsin dependent invasion is most likely independent of JAK signaling. Supporting this, a human whole kinome siRNA screen using the MCF7 p95ΔN-ErbB2 cells failed to show any role of JAK family members in the regulation of cysteine cathepsin activity (Rafn et al., 2012). A recent comprehensive study on the specificity of kinase inhibitors (Anastassiadis et al., 2011) shows that JAK3 inhibitor VI is not specific to JAKs but can additionally directly inhibit many kinases including few of the kinases earlier identified as regulators of ErbB2-induced invasion and increased expression and activity of cysteine cathepsins B and L (Rafn et al., 2012). These involve several members of the ERK-MAPK pathway including ERK2 as well as PKCα (Anastassiadis et al., 2011), all which may be contributing to the decreased *CTSL1* expression. Moreover, the decrease in the ErbB2 level that was induced by JAK3 inhibitor VI treatment could for example result from inhibition of ErbB2 recycling due to the capability of JAK3 inhibitor VI to inhibit PKCα. PKCα inhibition has been shown to block ErbB2 recycling in ErbB2-positive beast cancer cells (Magnifico et al., 2007; Rafn et al., 2012).

Gö6976 functions by competing for the ATP-binding sites of many kinases (Bain et al., 2007; Martiny-Baron and Fabbro, 2007). Among others, Gö6976 can inhibit calcium-dependent PKCα and PKCβ activation (Martiny-Baron and Fabbro, 2007; Martiny-Baron et al., 1993), of which the Gö6976-mediated inhibition of PKCα may contribute to its ability to inhibit ErbB2-induced invasion (Magnifico et al., 2007; Rafn et al., 2012). Roscovitine is a pan-selective inhibitor of Cdk1/2/5/7/9 and inhibits proliferative response by induction of cell cycle arrest in G$_1$ phase and apoptosis (Krystof et al., 2005; McClue et al., 2002). The effect of Roscovitine and Gö6976 on ErbB2-mediated pericellular distribution of the lysosomes was minor compared to lapatinib and JAK3 inhibitor VI. In an earlier study Gö6976 inhibition of PKCα was found to reduce invasion and ErbB2-mediated uPAR expression (Tan et al., 2006). In line with this, Gö6976 can inhibit tunnel formation in 3D collagen matrices, by a process that is regulated by a complex signaling network including PKCα (Fisher et al., 2009). Roscovitine can inhibit differentiation and invasion of metastatic melanoma cells (Mohapatra et al., 2007) and confers tumor suppressive effects in therapy-resistant breast cancer cells (Maggiorella et al., 2009; Nair et al., 2011). The (R)-enantiomer stereoisomer of Roscovitine (CYC-202/Seliciclib, Cyclacel Pharmaceuticals (Guzi, 2004)) is currently undergoing phase 2 clinical trials as a single-agent against non-small cell lung carcinoma and nasopharyngeal cancer and phase 1 clinical trials for the treatment of patients with advanced solid tumors in combination with Sapacitabine, a bioavailable pyrimidine analogue that targets DNA replication (Cyclacel Pharmaceuticals; http://cyclacel.com and clinical trials; http://clinicaltrials.gov). According to NCI (http://clinicaltrials.gov) neither, Gö6976 or JAK3 inhibitor VI are currently involved in clinical trials as anti-cancer agents.

We conclude that the screening procedure and the consequent verification analysis described here can be used to identify efficient novel inhibitors of ErbB2-induced cancer cell invasiveness. Since the screen is based on the detection of the drug-mediated inhibition of the oncogene-induced zFRase activity, it makes it also a promising method for identifying drugs that can specifically inhibit invasion mechanisms downstream of the ErbB2 receptor. Moreover, it can also be used for screening of invasion inhibitors for other types of cancers whose invasion depends on cysteine cathepsins and increased lysosomal activity. However, it is to be noted that the fluorescent nature of some compounds might require use of an alternative, colorimetric substrate. The screening procedure itself is simple and easy to automatize and thus it could be used to screen large amount of compounds quickly and cost efficiently. Especially interesting would be to screen libraries of compounds that have passed phase I clinical trials or compounds that are already in use in clinics to possibly facilitate discovery of novel inhibitors of invasion.

Appendix A.
Supplementary data

Supplementary data related to this article can be found at http://dx.doi.org/10.1016/j.molonc.2014.07.004.

REFERENCES

Adams, C., Aldous, D.J., Amendola, S., Bamborough, P., Bright, C., Crowe, S., Eastwood, P., Fenton, G., Foster, M., Harrison, T.K., King, S., Lai, J., Lawrence, C., Letallec, J.P., McCarthy, C., Moorcroft, N., Page, K., Rao, S., Redford, J., Sadiq, S., Smith, K., Souness, J.E., Thurairatnam, S., Vine, M., Wyman, B., 2003. Mapping the kinase domain of Janus Kinase 3. Bioorg. Med. Chem. Lett. 13, 3105–3110.

Anastassiadis, T., Deacon, S.W., Devarajan, K., Ma, H., Peterson, J.R., 2011. Comprehensive assay of kinase catalytic activity reveals features of kinase inhibitor selectivity. Nat. Biotechnol. 29, 1039–1045.

Arribas, J., Baselga, J., Pedersen, K., Parra-Palau, J.L., 2011. p95HER2 and breast cancer. Cancer Res. 71, 1515–1519.

Bain, J., Plater, L., Elliott, M., Shpiro, N., Hastie, C.J., McLauchlan, H., Klevernic, I., Arthur, J.S., Alessi, D.R., Cohen, P., 2007. The selectivity of protein kinase inhibitors: a further update. Biochem. J. 408, 297–315.

Baselga, J., Swain, S.M., 2009. Novel anticancer targets: revisiting ERBB2 and discovering ERBB3. Nat. Rev. Cancer 9, 463–475.

Blumenthal, G.M., Scher, N.S., Cortazar, P., Chattopadhyay, S., Tang, S., Song, P., Liu, Q., Ringgold, K., Pilaro, A.M., Tilley, A., King, K.E., Graham, L., Rellahan, B.L., Weinberg, W.C., Chi, B., Thomas, C., Hughes, P., Ibrahim, A., Justice, R., Pazdur, R., 2013. First FDA approval of dual anti-HER2 regimen: pertuzumab in combination with trastuzumab and docetaxel for HER2-positive metastatic breast cancer. Clin. Cancer Res. 19, 4911–4916.

Bosc, D.G., Goueli, B.S., Janknecht, R., 2001. HER2/Neu-mediated activation of the ETS transcription factor ER81 and its target gene MMP-1. Oncogene 20, 6215–6224.

Brix, D., Clemmensen, K., Kallunki, T., 2014. When good turns bad: regulation of invasion and metastasis by ErbB2 receptor tyrosine kinase. Cells 3, 53–78.

Chahrour, O., Cairns, D., Omran, Z., 2012. Small molecule kinase inhibitors as anti-cancer therapeutics. Mini Rev. Med. Chem. 12, 399–411.

Clynes, R.A., Towers, T.L., Presta, L.G., Ravetch, J.V., 2000. Inhibitory Fc receptors modulate in vivo cytotoxicity against tumor targets. Nat. Med. 6, 443–446.

Costa, A.G., Cusano, N.E., Silva, B.C., Cremers, S., Bilezikian, J.P., 2011. Cathepsin K: its skeletal actions and role as a therapeutic target in osteoporosis. Nat. Rev. Rheumatol. 7, 447–456.

De Keulenaer, G.W., Doggen, K., Lemmens, K., 2010. The vulnerability of the heart as a pluricellular paracrine organ: lessons from unexpected triggers of heart failure in targeted ErbB2 anticancer therapy. Circ. Res. 106, 35–46.

Dietrich, N., Thastrup, J., Holmberg, C., Gyrd-Hansen, M., Fehrenbacher, N., Lademann, U., Lerdrup, M., Herdegen, T., Jaattela, M., Kallunki, T., 2004. JNK2 mediates TNF-induced cell death in mouse embryonic fibroblasts via regulation of both caspase and cathepsin protease pathways. Cell Death Differ. 11, 301–313.

Egeblad, M., Mortensen, O.H., Jaattela, M., 2001. Truncated ErbB2 receptor enhances ErbB1 signaling and induces reversible, ERK-independent loss of epithelial morphology. Int. J. Cancer 94, 185–191.

Ellegaard, A.M., Groth-Pedersen, L., Oorschot, V., Klumperman, J., Kirkegaard, T., Nylandsted, J., Jaattela, M., 2013. Sunitinib and SU11652 inhibit acid sphingomyelinase, destabilize lysosomes, and inhibit multidrug resistance. Mol. Cancer Ther. 12, 2018–2030.

Farkas, T., Daugaard, M., Jaattela, M., 2011. Identification of small molecule inhibitors of phosphatidylinositol 3-kinase and autophagy. J. Biol. Chem. 286, 38904–38912.

Fehrenbacher, N., Bastholm, L., Kirkegaard-Sorensen, T., Rafn, B., Bottzauw, T., Nielsen, C., Weber, E., Shirasawa, S., Kallunki, T., Jaattela, M., 2008. Sensitization to the lysosomal cell death pathway by oncogene-induced down-regulation of lysosome-associated membrane proteins 1 and 2. Cancer Res. 68, 6623–6633.

Fisher, K.E., Sacharidou, A., Stratman, A.N., Mayo, A.M., Fisher, S.B., Mahan, R.D., Davis, M.J., Davis, G.E., 2009. MT1-MMP- and Cdc42-dependent signaling co-regulate cell invasion and tunnel formation in 3D collagen matrices. J. Cell Sci. 122, 4558–4569.

Ginestier, C., Hur, M.H., Charafe-Jauffret, E., Monville, F., Dutcher, J., Brown, M., Jacquemier, J., Viens, P., Kleer, C.G., Liu, S., Schott, A., Hayes, D., Birnbaum, D., Wicha, M.S., Dontu, G., 2007. ALDH1 is a marker of normal and malignant human mammary stem cells and a predictor of poor clinical outcome. Cell Stem Cell 1, 555–567.

Gocheva, V., Zeng, W., Ke, D., Klimstra, D., Reinheckel, T., Peters, C., Hanahan, D., Joyce, J.A., 2006. Distinct roles for cysteine cathepsin genes in multistage tumorigenesis. Genes & Development 20, 543–556.

Grant, S.K., 2009. Therapeutic protein kinase inhibitors. Cell. Mol. Life Sci. 66, 1163–1177.

Groth-Pedersen, L., Jaattela, M., 2013. Combating apoptosis and multidrug resistant cancers by targeting lysosomes. Cancer Lett. 332, 265–274.

Guzi, T., 2004. CYC-202 cyclacel. Curr. Opin. Investig. Drugs 5, 1311–1318.

Holbro, T., Beerli, R.R., Maurer, F., Koziczak, M., Barbas 3rd, C.F., Hynes, N.E., 2003. The ErbB2/ErbB3 heterodimer functions as an oncogenic unit: ErbB2 requires ErbB3 to drive breast tumor cell proliferation. Proc. Natl. Acad. Sci. U S A 100, 8933–8938.

Hynes, N.E., Lane, H.A., 2005. ERBB receptors and cancer: the complexity of targeted inhibitors. Nat. Rev. Cancer 5, 341–354.

Jensen, A.B., Wynne, C., Ramirez, G., He, W., Song, Y., Berd, Y., Wang, H., Mehta, A., Lombardi, A., 2010. The cathepsin K inhibitor odanacatib suppresses bone resorption in women with breast cancer and established bone metastases: results of a 4-week, double-blind, randomized, controlled trial. Clin. Breast Cancer 10, 452–458.

Kallunki, T., Olsen, O.D., Jaattela, M., 2013. Cancer-associated lysosomal changes: friends or foes? Oncogene 32, 1995–2004.

Ke, Z., Lin, H., Fan, Z., Cai, T.Q., Kaplan, R.A., Ma, C., Bower, K.A., Shi, X., Luo, J., 2006. MMP-2 mediates ethanol-induced invasion of mammary epithelial cells over-expressing ErbB2. Int. J. Cancer 119, 8–16.

Kedrin, D., Wyckoff, J., Boimel, P.J., Coniglio, S.J., Hynes, N.E., Arteaga, C.L., Segall, J.E., 2009. ERBB1 and ERBB2 have distinct functions in tumor cell invasion and intravasation. Clin. Cancer Res. 15, 3733–3739.

Kirkegaard, T., Jaattela, M., 2009. Lysosomal involvement in cell death and cancer. Biochim. Biophys. Acta 1793, 746–754.

Kobayashi, H., Ohi, H., Sugimura, M., Shinohara, H., Fujii, T., Terao, T., 1992. Inhibition of in vitro ovarian cancer cell invasion by modulation of urokinase-type plasminogen activator and cathepsin B. Cancer Res. 52, 3610–3614.

Kolwijck, E., Massuger, L.F., Thomas, C.M., Span, P.N., Krasovec, M., Kos, J., Sweep, F.C., 2010. Cathepsins B, L and cystatin C in cyst fluid of ovarian tumors. J. Cancer Res. Clin. Oncol. 136, 771−778.

Komurov, K., Tseng, J.T., Muller, M., Seviour, E.G., Moss, T.J., Yang, L., Nagrath, D., Ram, P.T., 2012. The glucose-deprivation network counteracts lapatinib-induced toxicity in resistant ErbB2-positive breast cancer cells. Mol. Syst. Biol. 8, 596.

Korkaya, H., Paulson, A., Iovino, F., Wicha, M.S., 2008. HER2 regulates the mammary stem/progenitor cell population driving tumorigenesis and invasion. Oncogene 27, 6120−6130.

Krystof, V., McNae, I.W., Walkinshaw, M.D., Fischer, P.M., Muller, P., Vojtesek, B., Orsag, M., Havlicek, L., Strnad, M., 2005. Antiproliferative activity of olomoucine II, a novel 2,6,9-trisubstituted purine cyclin-dependent kinase inhibitor. Cell. Mol. Life Sci. 62, 1763−1771.

Kumler, I., Tuxen, M.K., Nielsen, D.L., 2014. A systematic review of dual targeting in HER2-positive breast cancer. Cancer Treat. Rev. 40, 259−270.

Liang, K., Esteva, F.J., Albarracin, C., Stemke-Hale, K., Lu, Y., Bianchini, G., Yang, C.Y., Li, Y., Li, X., Chen, C.T., Mills, G.B., Hortobagyi, G.N., Mendelsohn, J., Hung, M.C., Fan, Z., 2010. Recombinant human erythropoietin antagonizes trastuzumab treatment of breast cancer cells via Jak2-mediated Src activation and PTEN inactivation. Cancer Cell 18, 423−435.

Maggiorella, L., Aubel, C., Haton, C., Milliat, F., Connault, E., Opolon, P., Deutsch, E., Bourhis, J., 2009. Cooperative effect of roscovitine and irradiation targets angiogenesis and induces vascular destabilization in human breast carcinoma. Cell Prolif. 42, 38−48.

Magnifico, A., Albano, L., Campaner, S., Campiglio, M., Pilotti, S., Menard, S., Tagliabue, E., 2007. Protein kinase Calpha determines HER2 fate in breast carcinoma cells with HER2 protein overexpression without gene amplification. Cancer Res. 67, 5308−5317.

Makhija, S., Amler, L.C., Glenn, D., Ueland, F.R., Gold, M.A., Dizon, D.S., Paton, V., Lin, C.Y., Januario, T., Ng, K., Strauss, A., Kelsey, S., Sliwkowski, M.X., Matulonis, U., 2010. Clinical activity of gemcitabine plus pertuzumab in platinum-resistant ovarian cancer, fallopian tube cancer, or primary peritoneal cancer. J. Clin. Oncol. 28, 1215−1223.

Martiny-Baron, G., Fabbro, D., 2007. Classical PKC isoforms in cancer. Pharmacol. Res. 55, 477−486.

Martiny-Baron, G., Kazanietz, M.G., Mischak, H., Blumberg, P.M., Kochs, G., Hug, H., Marme, D., Schachtele, C., 1993. Selective inhibition of protein kinase C isozymes by the indolocarbazole Go 6976. J. Biol. Chem. 268, 9194−9197.

McClue, S.J., Blake, D., Clarke, R., Cowan, A., Cummings, L., Fischer, P.M., MacKenzie, M., Melville, J., Stewart, K., Wang, S., Zhelev, N., Zheleva, D., Lane, D.P., 2002. In vitro and in vivo antitumor properties of the cyclin dependent kinase inhibitor CYC202 (R-roscovitine). Int. J. Cancer 102, 463−468.

Moasser, M.M., 2007. Targeting the function of the HER2 oncogene in human cancer therapeutics. Oncogene 26, 6577−6592.

Mohamed, M.M., Sloane, B.F., 2006. Cysteine cathepsins: multifunctional enzymes in cancer. Nat. Rev. Cancer 6, 764−775.

Mohapatra, S., Coppola, D., Riker, A.I., Pledger, W.J., 2007. Roscovitine inhibits differentiation and invasion in a three-dimensional skin reconstruction model of metastatic melanoma. Mol. Cancer Res. 5, 145−151.

Molina, M.A., Saez, R., Ramsey, E.E., Garcia-Barchino, M.J., Rojo, F., Evans, A.J., Albanell, J., Keenan, E.J., Lluch, A., Garcia-Conde, J., Baselga, J., Clinton, G.M., 2002. NH(2)-terminal truncated HER-2 protein but not full-length receptor is associated with nodal metastasis in human breast cancer. Clin. Cancer Res. 8, 347−353.

Nair, B.C., Vallabhaneni, S., Tekmal, R.R., Vadlamudi, R.K., 2011. Roscovitine confers tumor suppressive effect on therapy-resistant breast tumor cells. Breast Cancer Res. 13, R80.

Nevalainen, M.T., Xie, J., Torhorst, J., Bubendorf, L., Haas, P., Kononen, J., Sauter, G., Rui, H., 2004. Signal transducer and activator of transcription-5 activation and breast cancer prognosis. J. Clin. Oncol. 22, 2053−2060.

Nishikawa, H., Ozaki, Y., Nakanishi, T., Blomgren, K., Tada, T., Arakawa, A., Suzumori, K., 2004. The role of cathepsin B and cystatin C in the mechanisms of invasion by ovarian cancer. Gynecol. Oncol. 92, 881−886.

Olayioye, M.A., Beuvink, I., Horsch, K., Daly, J.M., Hynes, N.E., 1999. ErbB receptor-induced activation of stat transcription factors is mediated by Src tyrosine kinases. J. Biol. Chem. 274, 17209−17218.

Pena-Llopis, S., Vega-Rubin-de-Celis, S., Schwartz, J.C., Wolff, N.C., Tran, T.A., Zou, L., Xie, X.J., Corey, D.R., Brugarolas, J., 2011. Regulation of TFEB and V-ATPases by mTORC1. EMBO J. 30, 3242−3258.

Perez, E.A., Koehler, M., Byrne, J., Preston, A.J., Rappold, E., Ewer, M.S., 2008. Cardiac safety of lapatinib: pooled analysis of 3689 patients enrolled in clinical trials. Mayo Clin. Proc. 83, 679−686.

Pfaffl, M.W., 2001. A new mathematical model for relative quantification in real-time RT-PCR. Nucleic Acids Res. 29, e45.

Rafn, B., Nielsen, C.F., Andersen, S.H., Szyniarowski, P., Corcelle-Termeau, E., Valo, E., Fehrenbacher, N., Olsen, C.J., Daugaard, M., Egebjerg, C., Bottzauw, T., Kohonen, P., Nylandsted, J., Hautaniemi, S., Moreira, J., Jaattela, M., Kallunki, T., 2012. ErbB2-driven breast cancer cell invasion depends on a complex signaling network activating myeloid zinc finger-1-dependent cathepsin B expression. Mol. Cell 45, 764−776.

Ren, Z., Schaefer, T.S., 2002. ErbB-2 activates Stat3 alpha in a Src- and JAK2-dependent manner. J. Biol. Chem. 277, 38486−38493.

Santarius, T., Shipley, J., Brewer, D., Stratton, M.R., Cooper, C.S., 2010. A census of amplified and overexpressed human cancer genes. Nat. Rev. Cancer 10, 59−64.

Scaltriti, M., Chandarlapaty, S., Prudkin, L., Aura, C., Jimenez, J., Angelini, P.D., Sanchez, G., Guzman, M., Parra, J.L., Ellis, C., Gagnon, R., Koehler, M., Gomez, H., Geyer, C., Cameron, D., Arribas, J., Rosen, N., Baselga, J., 2010. Clinical benefit of lapatinib-based therapy in patients with human epidermal growth factor receptor 2-positive breast tumors coexpressing the truncated p95HER2 receptor. Clin. Cancer Res. 16, 2688−2695.

Scaltriti, M., Rojo, F., Ocana, A., Anido, J., Guzman, M., Cortes, J., Di Cosimo, S., Matias-Guiu, X., Ramon y Cajal, S., Arribas, J., Baselga, J., 2007. Expression of p95HER2, a truncated form of the HER2 receptor, and response to anti-HER2 therapies in breast cancer. J. Natl. Cancer Inst. 99, 628−638.

Settembre, C., Di Malta, C., Polito, V.A., Garcia Arencibia, M., Vetrini, F., Erdin, S., Erdin, S.U., Huynh, T., Medina, D., Colella, P., Sardiello, M., Rubinsztein, D.C., Ballabio, A., 2011. TFEB links autophagy to lysosomal biogenesis. Science 332, 1429−1433.

Settembre, C., Fraldi, A., Medina, D.L., Ballabio, A., 2013. Signals from the lysosome: a control centre for cellular clearance and energy metabolism. Nat. Rev. Mol. Cell Biol. 14, 283−296.

Slamon, D.J., Godolphin, W., Jones, L.A., Holt, J.A., Wong, S.G., Keith, D.E., Levin, W.J., Stuart, S.G., Udove, J., Ullrich, A., et al., 1989. Studies of the HER-2/neu proto-oncogene in human breast and ovarian cancer. Science 244, 707−712.

Slamon, D.J., Leyland-Jones, B., Shak, S., Fuchs, H., Paton, V., Bajamonde, A., Fleming, T., Eiermann, W., Wolter, J., Pegram, M., Baselga, J., Norton, L., 2001. Use of chemotherapy plus a monoclonal antibody against HER2 for metastatic

breast cancer that overexpresses HER2. N. Engl. J. Med. 344, 783–792.

Sloane, B.F., Moin, K., Sameni, M., Tait, L.R., Rozhin, J., Ziegler, G., 1994. Membrane association of cathepsin B can be induced by transfection of human breast epithelial cells with c-Ha-ras oncogene. J. Cell Sci. 107 (Pt 2), 373–384.

Strauss, R., Li, Z.Y., Liu, Y., Beyer, I., Persson, J., Sova, P., Moller, T., Pesonen, S., Hemminki, A., Hamerlik, P., Drescher, C., Urban, N., Bartek, J., Lieber, A., 2011. Analysis of epithelial and mesenchymal markers in ovarian cancer reveals phenotypic heterogeneity and plasticity. PloS One 6, e16186.

Sultan, A.S., Xie, J., LeBaron, M.J., Ealley, E.L., Nevalainen, M.T., Rui, H., 2005. Stat5 promotes homotypic adhesion and inhibits invasive characteristics of human breast cancer cells. Oncogene 24, 746–760.

Tan, M., Li, P., Sun, M., Yin, G., Yu, D., 2006. Upregulation and activation of PKC alpha by ErbB2 through Src promotes breast cancer cell invasion that can be blocked by combined treatment with PKC alpha and Src inhibitors. Oncogene 25, 3286–3295.

Thomssen, C., Schmitt, M., Goretzki, L., Oppelt, P., Pache, L., Dettmar, P., Janicke, F., Graeff, H., 1995. Prognostic value of the cysteine proteases cathepsins B and cathepsin L in human breast cancer. Clin. Cancer Res. 1, 741–746.

Vasiljeva, O., Papazoglou, A., Kruger, A., Brodoefel, H., Korovin, M., Deussing, J., Augustin, N., Nielsen, B.S., Almholt, K., Bogyo, M., Peters, C., Reinheckel, T., 2006. Tumor cell-derived and macrophage-derived cathepsin B promotes progression and lung metastasis of mammary cancer. Cancer Res. 66, 5242–5250.

Victor, B.C., Sloane, B.F., 2007. Cysteine cathepsin non-inhibitory binding partners: modulating intracellular trafficking and function. Biol. Chem. 388, 1131–1140.

Ward, T.M., Iorns, E., Liu, X., Hoe, N., Kim, P., Singh, S., Dean, S., Jegg, A.M., Gallas, M., Rodriguez, C., Lippman, M., Landgraf, R.,

Pegram, M.D., 2013. Truncated p110 ERBB2 induces mammary epithelial cell migration, invasion and orthotopic xenograft formation, and is associated with loss of phosphorylated STAT5. Oncogene 33 (19), 2463–2474.

Xia, W., Liu, Z., Zong, R., Liu, L., Zhao, S., Bacus, S.S., Mao, Y., He, J., Wulfkuhle, J.D., Petricoin 3rd, E.F., Osada, T., Yang, X.Y., Hartman, Z.C., Clay, T.M., Blackwell, K.L., Lyerly, H.K., Spector, N.L., 2011. Truncated ErbB2 expressed in tumor cell nuclei contributes to acquired therapeutic resistance to ErbB2 kinase inhibitors. Mol. Cancer Ther. 10, 1367–1374.

Yamaoka, K., Saharinen, P., Pesu, M., Holt 3rd, V.E., Silvennoinen, O., O'Shea, J.J., 2004. The Janus kinases (Jaks). Genome Biol. 5, 253.

Yamauchi, T., Yamauchi, N., Ueki, K., Sugiyama, T., Waki, H., Miki, H., Tobe, K., Matsuda, S., Tsushima, T., Yamamoto, T., Fujita, T., Taketani, Y., Fukayama, M., Kimura, S., Yazaki, Y., Nagai, R., Kadowaki, T., 2000. Constitutive tyrosine phosphorylation of ErbB-2 via Jak2 by autocrine secretion of prolactin in human breast cancer. J. Biol. Chem. 275, 33937–33944.

Yong, H.Y., Kim, I.Y., Kim, J.S., Moon, A., 2010. ErbB2-enhanced invasiveness of H-Ras MCF10A breast cells requires MMP-13 and uPA upregulation via p38 MAPK signaling. Int. J. Oncol. 36, 501–507.

Yu, D., Wolf, J.K., Scanlon, M., Price, J.E., Hung, M.C., 1993. Enhanced c-erbB-2/neu expression in human ovarian cancer cells correlates with more severe malignancy that can be suppressed by E1A. Cancer Res. 53, 891–898.

Zhang, W., Yang, H.C., Wang, Q., Yang, Z.J., Chen, H., Wang, S.M., Pan, Z.M., Tang, B.J., Li, Q.Q., Li, L., 2011. Clinical value of combined detection of serum matrix metalloproteinase-9, heparanase, and cathepsin for determining ovarian cancer invasion and metastasis. Anticancer Res. 31, 3423–3428.